Investigation of Unsteady Subsonic Spoiler and Flap Aerodynamics

M. Costes,* A. Gravelle,† and J. J. Philippe*
Office National d'Etudes et de Recherches Aérospatiales, Châtillon, France
S. Vogel‡
Messerschmidt-Bölkow-Blohm Gmbtt, Bremen, Federal Republic of Germany
and
H. Triebstein§
Deutsche Forschungs-und Versuchsanstalt für Luft-und Raumfahrt e. V. Göttingen, Federal Republic of Germany

An experimental study has been performed in the ONERA F1 pressurized wind tunnel on a 1-m chord supercritical airfoil equipped with a spoiler and a flap in a two-dimensional flow. Both the spoiler and the flap can be steadily deflected simultaneously, and one control surface can then be driven with a harmonic motion, a white noise motion, or a ramp motion for various rise times. The steady and unsteady pressures, and the lift and moment coefficients depend on Reynolds number, mean steady deflection, and frequency. The interaction between the control surfaces is examined. Unsteady pressure time histories for ramp-type motions for various rise times and initial deflections are also given. Finally, some comparisons are presented between a theoretical method developed at ONERA and the experimental data for a steady deflected spoiler.

Nomenclature

c = airfoil chord
C_D = drag coefficient
C_L = lift coefficient
C_M = moment coefficient at quarter-chord
$C_M\delta$ = unsteady moment coefficient, first harmonic
C_N = normal force coefficient
$C_N\delta$ = unsteady normal force coefficient, first harmonic
C_p = unsteady pressure coefficient: $[p(t)-p_0]/(\frac{1}{2}\rho V^2\delta_i)$
C_{p1} = unsteady pressure coefficient, first harmonic
f = oscillation frequency
H = harmonic excitation
k = reduced frequency = $\pi fc/V$
K_p = steady pressure coefficient
M = freestream Mach number
p_i = stagnation pressure
p_0 = mean static pressure (unsteady flow)
$p(t)$ = unsteady pressure
Re = Reynolds number based on the chord
t = time
V = freestream velocity
WN = white noise excitation
x = chordwise position
α = angle of attack
δ = spoiler deflection (ramp movement)
δ_f = flap deflection
δ_i = oscillation amplitude
δ_{sp} = spoiler deflection
ϕ_1 = phase angle, first harmonic
η = flap deflection (ramp movement)
ρ = freestream density

Received Dec. 11, 1986; revision received Jan. 31, 1987.

*Research Engineer, Aerodynamic Department.
†Research Engineer, Structure Department.
‡Dipl. Eng., Aeroelastic Department.
§Senior Scientist, Institute of Aeroelasticity.

Introduction

THE development of active control technology has involved a special interest in control surface unsteady aerodynamics. From the computational point of view, the numerical codes available for calculating unsteady aerodynamics have for a long time been linear methods. An important effort has been under way for about ten years to develop more accurate codes. But most of these methods remain inviscid ones and, consequently, they are unable to calculate the viscous effects on the flap characteristics or the separated flow induced by a spoiler, even in steady flows.

These facts indicate the need to evaluate the steady and unsteady performances of spoilers and flaps from experimental data. An experimental study has been carried out with a two-dimensional model equipped with a spoiler and a flap. The goals of this study were to improve knowlege of the aerodynamic forces induced by the steady or unsteady deflection of spoilers and flaps and to obtain accurate measurements necessary to validate the prediction codes that are being developed.

Test Facilities and Model

The model was tested in the ONERA low-speed pressurized wind tunnel F1. It was set up between two walls erected in the test section in order to assure two-dimensional tests.

The wing (Fig. 1) is a rectangular supercritical wing of 2-m span by 1-m chord. The three components are the main box, which can rotate around an axis located at 27.5% of the chord for an angle of attack change, the spoiler, 2×0.15 m, which can rotate from $\delta_{sp}=0$ to 31 deg around the hinge line located at 67% of the chord, and the flap, 2×0.125 m, which can

move from $\delta_f = -5$ deg (upward) to $\delta_f = +10$ deg (downward) around its hinge line located at around 87.5% of the chord.

The model was equipped with 115 static pressure tappings along one middle and two lateral sections, 115 unsteady pressure pickups with the same chordwise distribution, 13 accelerometers, and four strain gage bridges. The angle of attack was fixed manually, whereas the spoiler and flap were hydraulically actuated by a feedback servosystem. The unsteady data acquisition equipment used is described in Ref. 1.

The test program included, for each control surface, the study of the mean deflection, oscillation amplitude, reduced frequency, and Reynolds number for a harmonic excitation. Furthermore, the interaction between the two control surfaces (the influence of a control surface static deflection on the other control efficiency) was examined. Finally, several white noise and "ramp" excitations were used. The test program involved about 120 steady and 160 unsteady configurations. All of the tests were performed at $M = 0.2$. The main configurations were systematically tested at a stagnation pressure equal to 1 bar corresponding to a Reynolds number of about 4 million and at a stagnation pressure equal to 4 bars corresponding to a Reynolds number of about 16 million.

This paper is mainly concerned with the influence of the Reynolds number on control surface efficiency, the comparison between spoiler and flap characteristics, and the study of the interaction between control surfaces (spoiler and flap) in steady and unsteady configurations. Examples of the ramp measurements are also given. Finally, the computer code[2] to calculate the steady flow around an airfoil equipped with a spoiler is presented, and some comparisons with experimental data are made.

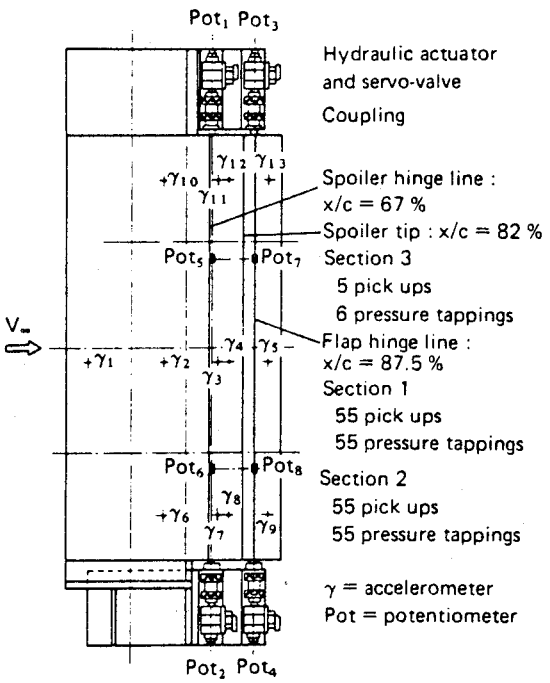

Fig. 1 Model wing.

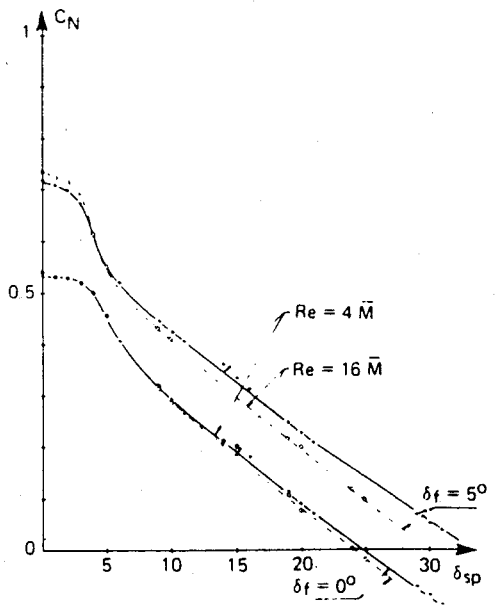

Fig. 2 Airfoil with spoiler: steady Reynolds effect.

Reynolds Number Effect

Steady Configuration

Figure 2 shows the normal force vs spoiler deflection calculated from the pressure integration for two Reynolds numbers (4 and 16 million) and for two flap angles. For $\delta_f = 5$ deg, at low spoiler deflections, the normal force is greater at

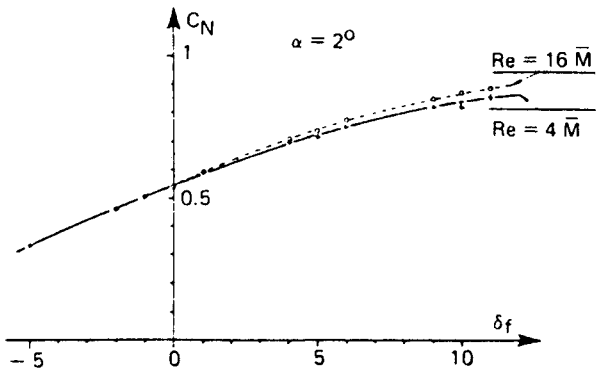

Fig. 3 Airfoil with flap: steady Reynolds effect.

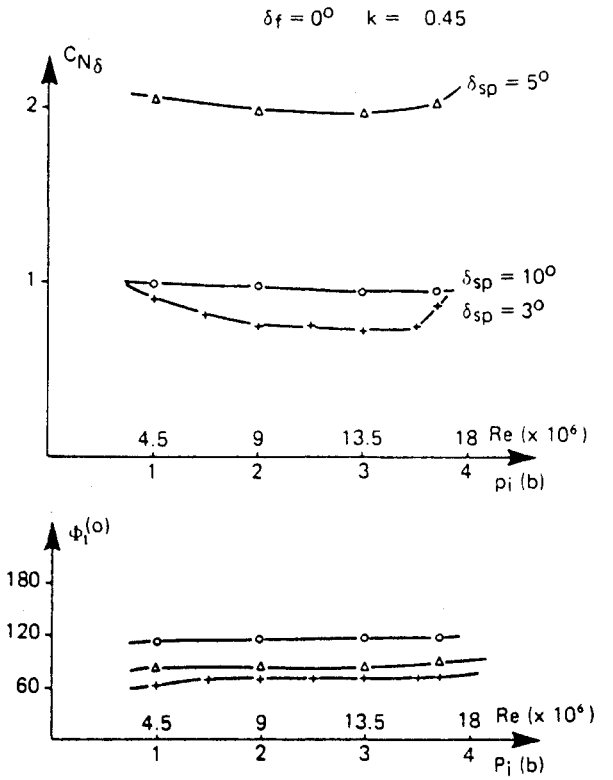

Fig. 4 Oscillating spoiler: influence of Reynolds number on the lift coefficient.

$Re = 16 \times 10^6$ than at $Re = 4 \times 10^6$. This is due to a better flap efficiency at high Reynolds numbers, where viscous effects are less important, as proved by Fig. 3. On the other hand, for high spoiler deflections, the normal forces are lower at $Re = 16 \times 10^6$ than at $Re = 4 \times 10^6$, which shows that the spoiler efficiency is greater in this situation. The boundary-layer thickness is lower on the spoiler and in front of it, and this may induce a greater effective spoiler angle. However, the conclusions on the Reynolds number influence may be erroneous because of its weakness and the possible spoiler deformations that can appear when the stagnation pressure is increased.

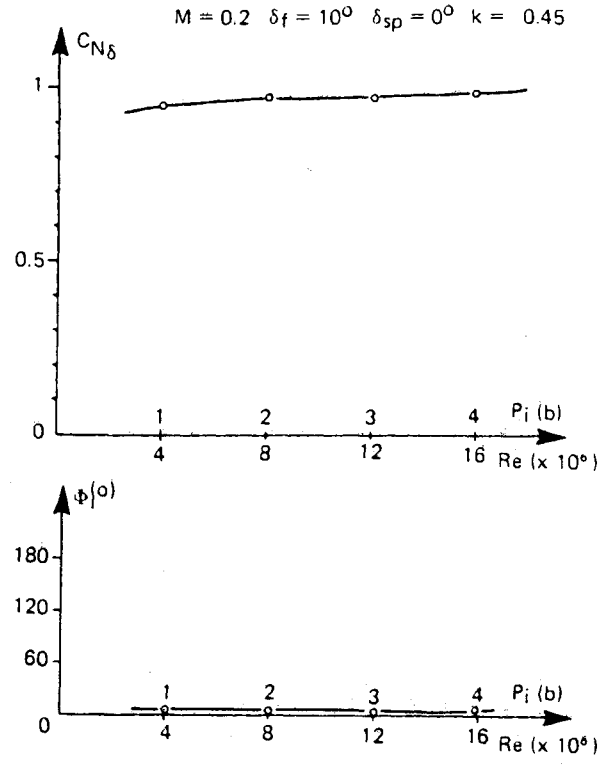

Fig. 5 Oscillating flap: influence of Reynolds number on the lift coefficient.

Unsteady Configurations

Figure 4 shows the Reynolds number effect on the spoiler efficiency. For small spoiler deflections ($\delta_{sp} = 3$ deg/5 deg), a noticeable variation can be seen with a minimum for $Re \simeq 13.5 \times 10^6$. The two main Reynolds numbers tested (4.5×10^6 and 18×10^6) yield virtually the same results. Then, when the spoiler deflection is increased ($\delta_{sp} = 10$ deg), this influence can no longer be detected: the reattachment point downstream of the spoiler is too far in the wake to have an effect on the unsteady lift. Finally, it must be noted that practically no effect can be seen on the phases.

For the flap, as illustrated in Fig. 5, the efficiency increases slowly with the Reynolds number, but this effect is very weak. This is in good agreement with steady measurements.

Comparison Between Spoiler and Flap Efficiencies

Influence of Mean Deflection

Figure 6 shows the unsteady pressures (first harmonic) measured on the airfoil for several spoiler deflections. The curve of the pressure distribution has a typical shape, with the pressure distribution strongly depending on the mean deflection. The unsteady pressures generated by the spoiler motion are maximum for a spoiler angle of 5 deg, when the separated flow zone, induced by the spoiler, reaches the airfoil trailing edge. For a spoiler deflection greater than 10 deg, the unsteady pressure level remains quite constant. The phase evolution is more regular with a diminution of the phase lag with an increasing mean spoiler deflection.

The unsteady pressure distributions for the flap (Fig. 7) reveal a continuous decrease of the amplitudes and of the phase lag when the flap deflection increases. This is due to the occurrence of greater viscous effects, and more particularly to the appearance of trailing edge separation, which is obviously present at $\delta_f = 10$ deg.

A comparison of the spoiler and flap efficiencies can be seen in Fig. 8. This efficiency is defined here as the unsteady lift capability (the modulus of the first harmonic). As expected from the unsteady pressure distribution curves, the unsteady forces (C_N as well as C_M) present far less variation for the flap than for the spoiler at "low" steady deflections, and the phase lag is also generally much smaller for the flap. A spoiler allows high unsteady forces for small deflections and could be quite realistic for applications because small spoiler angles don't in-

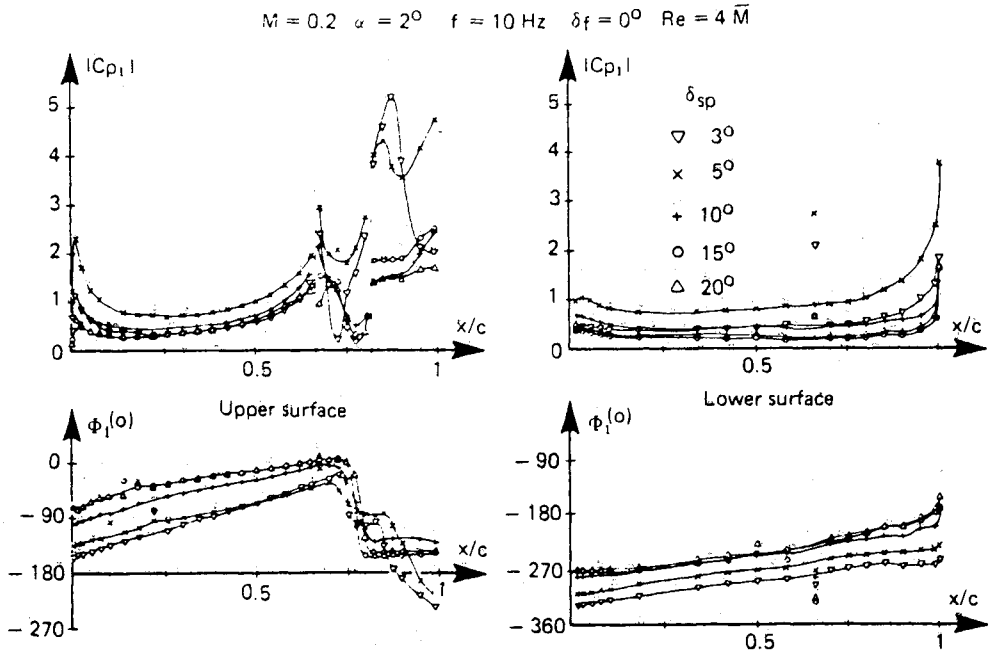

Fig. 6 Oscillating spoiler: influence of spoiler deflection.

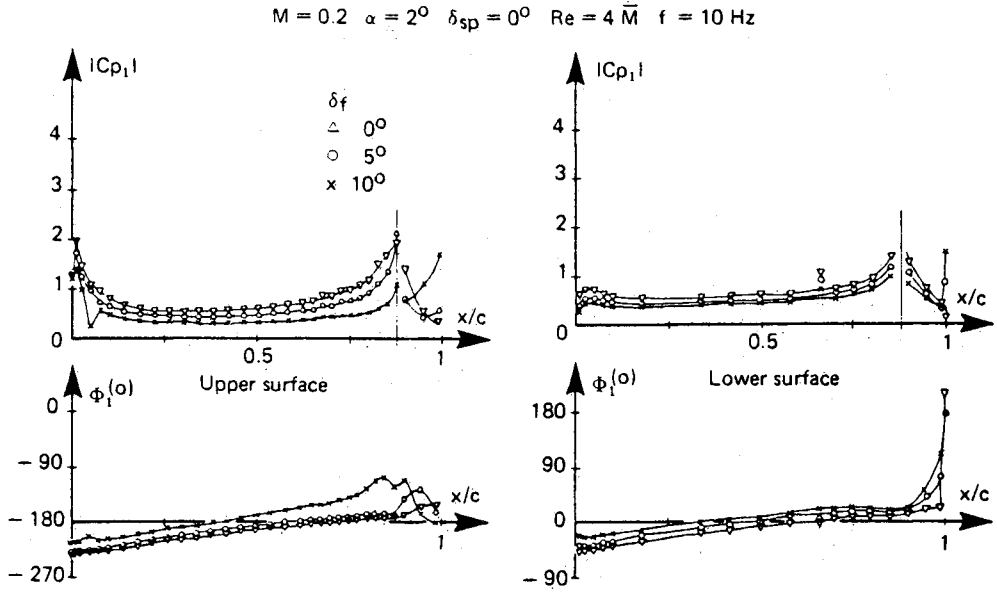

Fig. 7 Oscillating flap: influence of flap deflection.

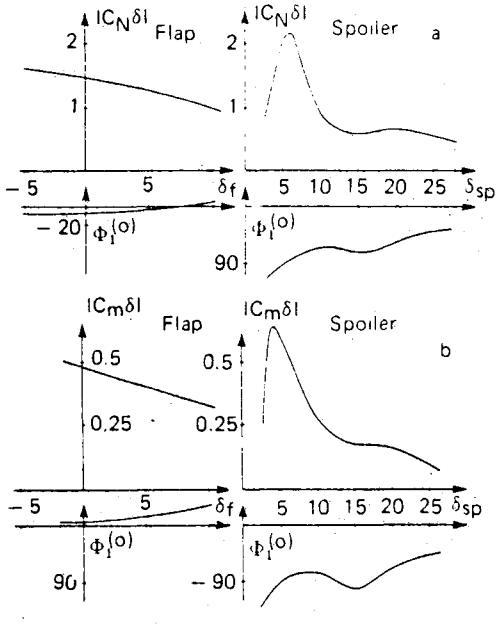

Fig. 8 Comparison between spoiler and flap: influence of mean deflection.

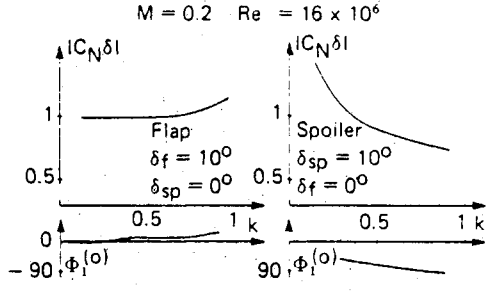

Fig. 9 Comparison between spoiler and flap: influence of reduced frequency.

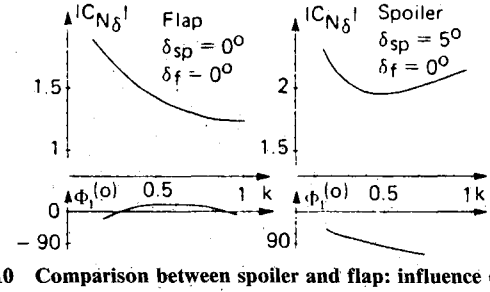

Fig. 10 Comparison between spoiler and flap: influence of reduced frequency.

duce too severe a drag penalty. However, good efficiency is obtained with quite large phase lags, the order of which is about 80–90 deg. Finally, it should be noted that the results on the modulus are in good agreement with the steady results previously seen (Fig. 2 and 3).

Influence of the Reduced Frequency

For the same efficiency level for both the spoiler and the flap, Fig. 9 shows the influence of the reduced frequency on the lift coefficient. The flap unsteady lift increases slightly at high reduced frequencies, and the spoiler efficiency strongly decreases with the frequency. In the region of greatest efficiency for each control surface (Fig. 10), the results are quite different. For the flap, the lift coefficient decreases significantly with the frequency; for the spoiler, the lift begins to decrease, but from $k \sim 0.5$, it increases regularly with the reduced frequency. Consequently, the effect of frequency strongly depends on the mean flow conditions.

Aerodynamic Interaction Between Control Surfaces

Spoiler Efficiency vs Flap Deflection

Figure 11 shows the spoiler steady efficiency curve for several flap deflections. The efficiency is defined as the lift loss capability given by the spoiler. The curve shape is quite classical, with a nonlinear zone for small spoiler deflections where the control surface has practically no efficiency. This nonlinear zone is reduced as the flap angle is increased. For great spoiler deflections, the normal force curve slope doesn't depend on the flap deflection, but the lift loss is obviously greater for high flap angles because the spoiler nonlinear zone is shorter. This phenomenon can be explained by looking at the airfoil pressure distribution (Figs. 12 and 13). For small spoiler deflections, the flow that is separated at the spoiler tip reattaches before the trailing edge, and the spoiler is only a local disturbance in the flow since no effect can be seen on the lower surface or on the upper surface in front of it (until

$\delta_{sp} = 3$ deg in Fig. 12 and 6 deg in Fig. 13). The spoiler deflection effect can be felt elsewhere only when the separated zone has reached the wake, inducing then a completely new pressure distribution and consequently a significant lift loss (from $\delta_{sp} = 7$ deg/8 deg when $\delta_f = 5$ deg and from $\delta_{sp} = 4$ deg/5 deg for $\delta_f = 5$ deg).

For the unsteady case, the same analysis can be made. For $\delta_{sp} = 3$ deg (Fig. 14), the influence of the flap deflection on the unsteady pressures is very important, with a pressure level decreasing when the flap deflection decreases. On the other hand, for $\delta_{sp} = 20$ deg (Fig. 15), the unsteady pressures are exactly the same for all of the flap deflections, except on the lower side phases. Consequently, there results a constant unsteady lift capability that becomes obvious when one looks at the steady curve given in Fig. 11.

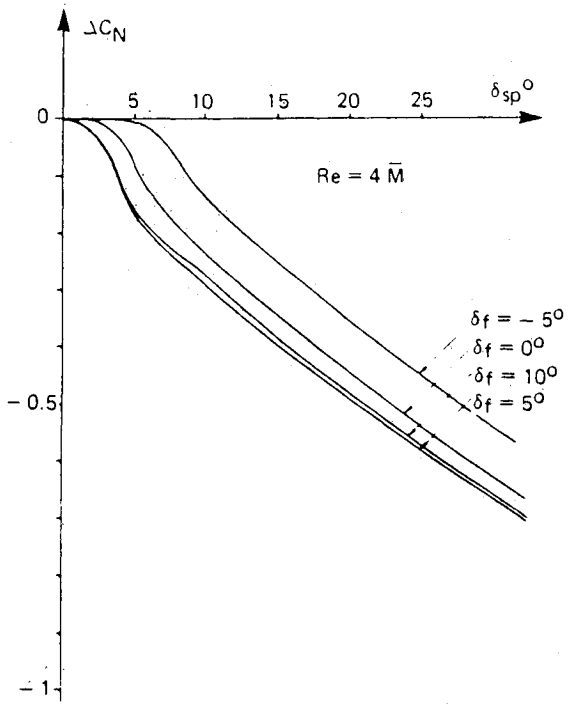

Fig. 11 Influence of flap deflection on spoiler efficiency.

Flap Efficiency vs Spoiler Deflection

For steady configurations, Fig. 16 shows that the spoiler mean deflection influences the flap efficiency only for $\delta_{sp} = 5$ deg, i.e., when the flow behind the spoiler is not fully separated. For greater spoiler deflections, the flap moves in a separated flow, but the curves C_N (δ_{sp}) and C_M (δ_{sp}) become more linear and the lift and moment curve shapes are the same, whatever the spoiler angle may be. This efficiency is, however, lower than in the case without spoiler erected.

For the oscillating flap (Fig. 17), the unsteady pressure remains quite constant from $\delta_{sp} = 10$ deg except on the flap itself. Otherwise, it is not obvious that unsteady pressures must be the same when pure harmonic and white noise excitations are performed on a flap in a separated flow region. A large loss of efficiency as well as a mean phase shift of about 20 deg appears when the spoiler deflection is increased from 0 to 10 deg. This point has to be taken into account if active controls are applied to flaps: the gain and phase margins of such controls must be large enough to be stable in all configurations. Finally, the aerodynamics interaction between control surfaces appears to be very important for this two-dimensional case, but it can be expected to be smaller for actual three-dimensional configurations.[4]

Ramp-Type Excitation of Spoiler and Flap

Because spoilers behave nonlinearly, especially for small deflections, additional investigations are necessary for other time history motions representative of flight conditions. Consequently, ramp-like motions represented by

$$\delta(t) = \delta_0 + \frac{1}{2}(\delta_{max} - \delta_0)\left[1 - \cos\left(\pi \frac{t - t_0}{t_1 - t_0}\right)\right] \quad t_0 < t < t_1$$

$$= \delta_{max} \quad t_1 < t < t_2$$

$$= \delta_0 + \frac{1}{2}(\delta_{max} - \delta_0)\left[1 + \cos\left(\pi \frac{t - t_2}{t_3 - t_2}\right)\right] \quad t_2 < t < t_3$$

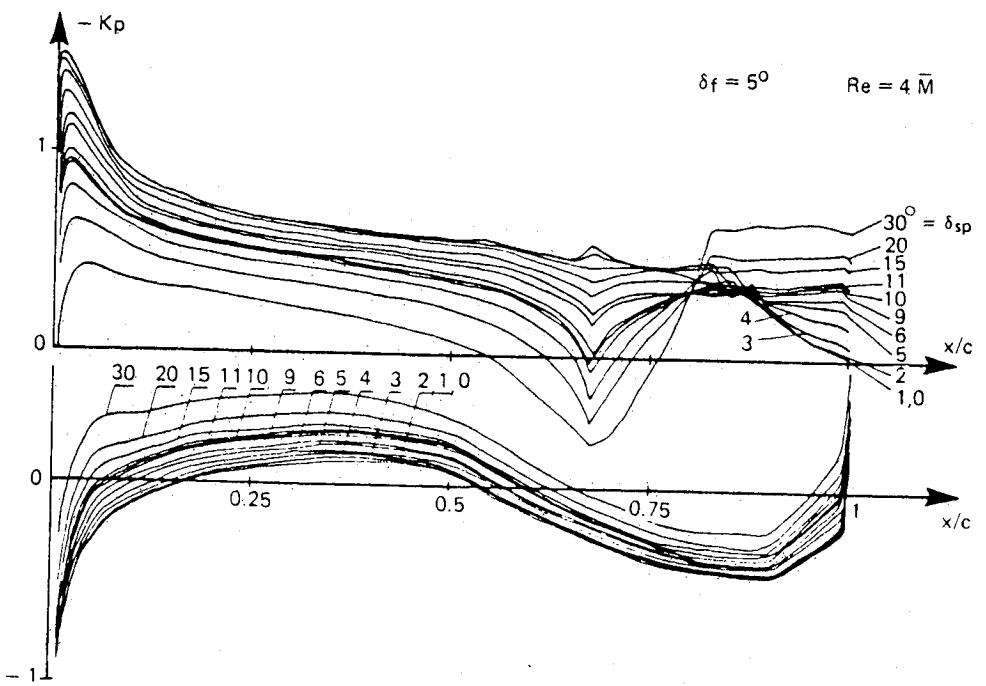

Fig. 12 Steady pressure distributions vs spoiler deflection for 5 deg flap angle.

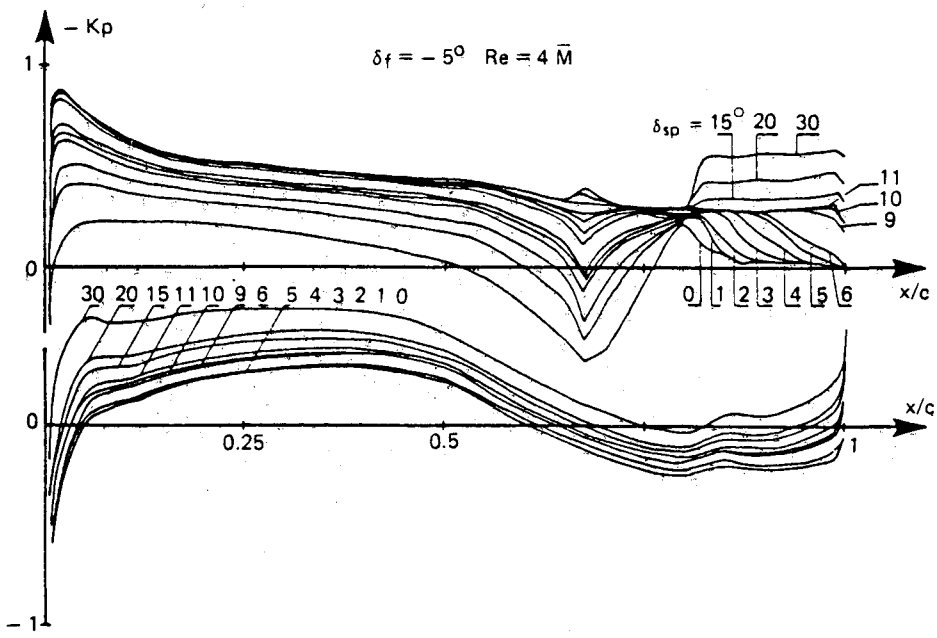

Fig. 13 Steady pressure distributions vs spoiler deflection for −5 deg flap angle.

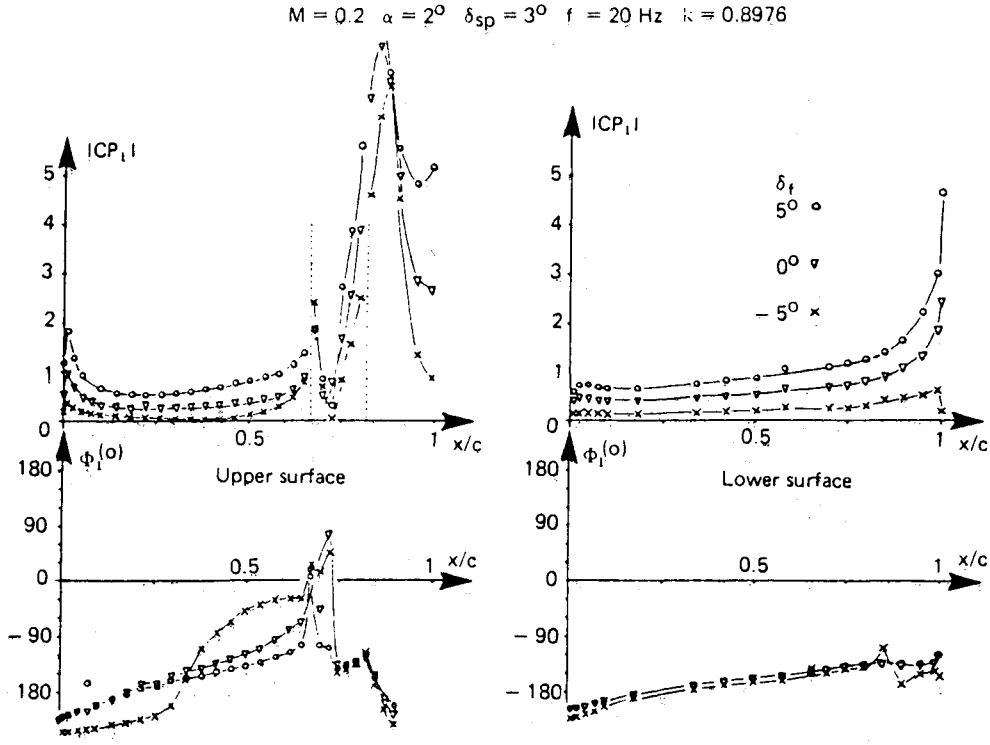

Fig. 14 Oscillating spoiler: influence of flap deflection.

have also been used for spoiler and flap excitation. The parameters examined were the starting deflection δ_0, its maximum value δ_{max}, and the deflection rate $\dot{\delta}$. The relation between the time corner points was $(t_1-t_0,\ t_2-t_1,\ t_3-t_2)=(1,2,1)$.

Figure 18 shows some selected pressure time histories measured on the airfoil for a spoiler ramp motion. The pressure response is nonlinear only on the rear part of the spoiler and behind it, i.e., where separated flows can occur during the spoiler motion. These nonlinearities are larger when the deflection starts from $\delta_0=0$ deg, and they increase with the deflection rate. On the rear part of the spoiler, the pressure at the starting phase gives opposite values compared to static ones. Behind the spoiler, the pressures start also with small opposite values, but they turn suddenly into a large overshoot. This behavior can also be seen below the spoiler for fast motions.

This adverse behavior can be seen on the lift and moment coefficients (Fig. 19). The nonlinear effect is more important on the moment coefficient because the nonlinearities appear mainly on the rear part of the airfoil upper surface. A response lag can also be seen for both coefficients. At last, the adverse effect is smaller when the erection starts with positive spoiler deflections or when the deflection rate is getting smaller. In this case, the response lag also decreases.

For a flap ramp motion (Fig. 20), no adverse effect appears, but a slight overshoot is still present.

Comparison Between Steady Computations and Experiment

A computer code based on strong viscous-inviscid interaction has been developed by J. C. Le Balleur.[2,3] Its ability to take into account strong viscous effects and, consequently, separated flows has led to the development of a spoiler ap-

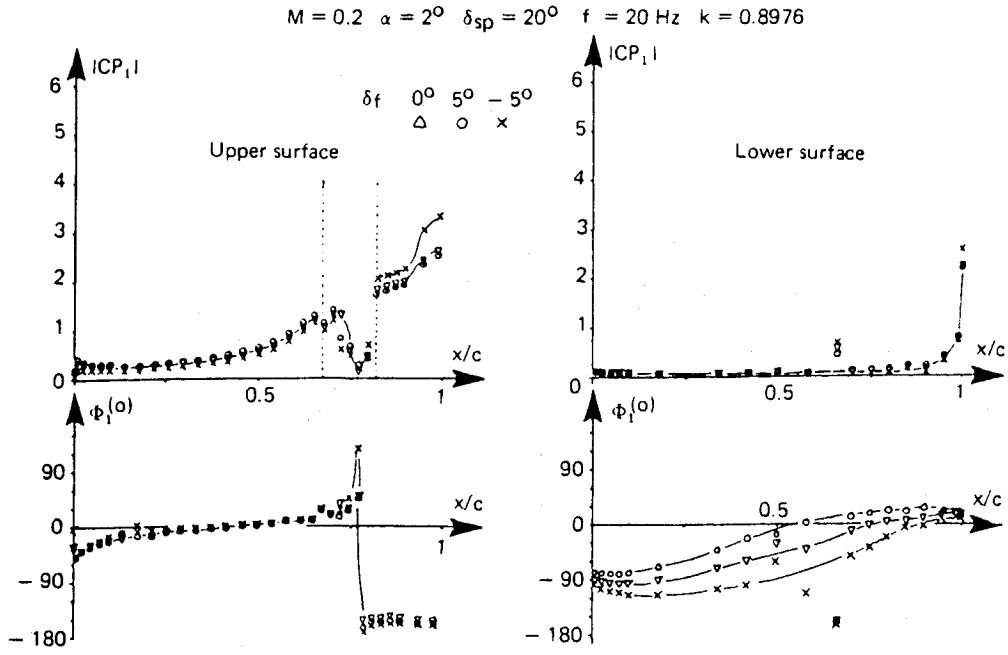

Fig. 15 Oscillating spoiler: influence of flap deflection.

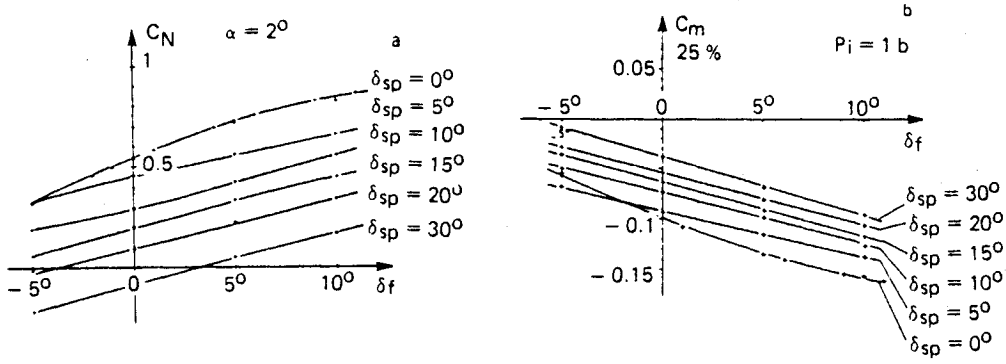

Fig. 16 Influence of spoiler deflection on the flap efficiency.

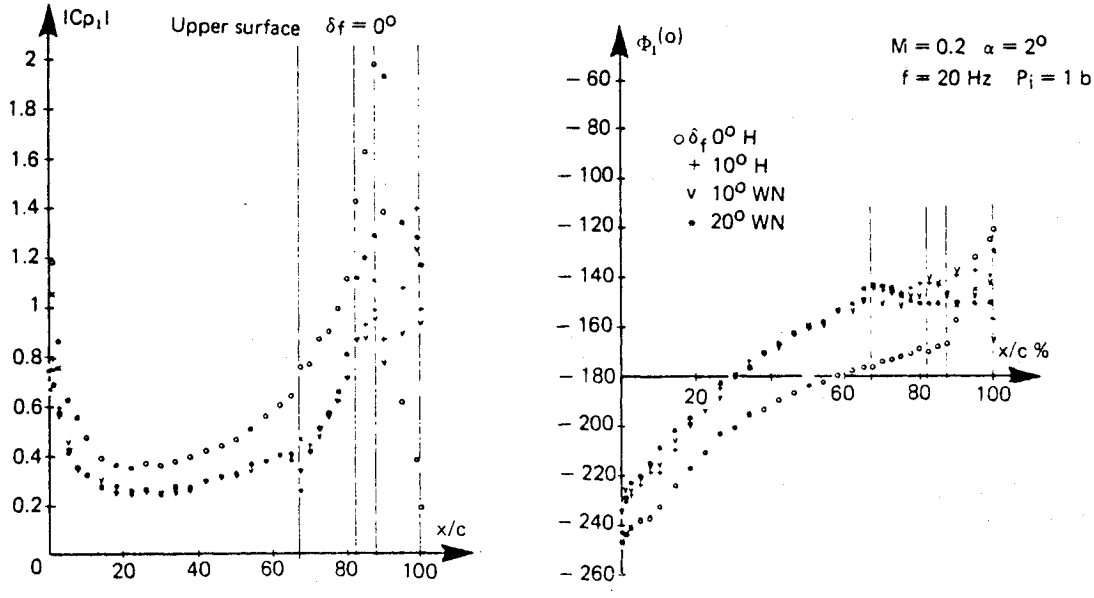

Fig. 17 Oscillating flap: influence of spoiler deflection.

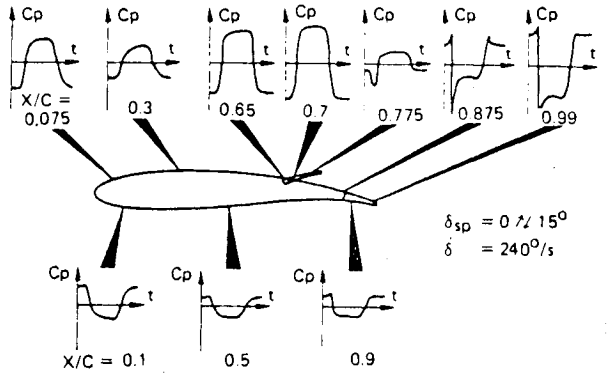

Fig. 18 Time history pressure distribution for a spoiler ramp movement.

plication. The main characteristics of the code are a strong coupling method in a direct or semi-inverse mode, assured between the inviscid flow, calculated from the full potential equation written in a conservative form, and the viscous region, calculated from integral equations of a defect formulation. The spoiler is modeled by changing the boundary conditions on the airfoil as in small perturbation techniques: the slope at the wall is increased by the spoiler deflection in the spoiler region, and a jump equal to the spoiler height is imposed to the displacement thickness at the spoiler tip.

This code has been used for some configurations tested in the F1 wind tunnel. Figure 21 shows good agreement between computed and measured pressures for $\delta_{sp} = 0/10$ deg for the two extreme Reynolds numbers tested. In Fig. 22, the evolution of the integrated coefficients (lift and moment) vs the spoiler deflection for $\delta_f = -5/0/5/10$ deg is plotted. The

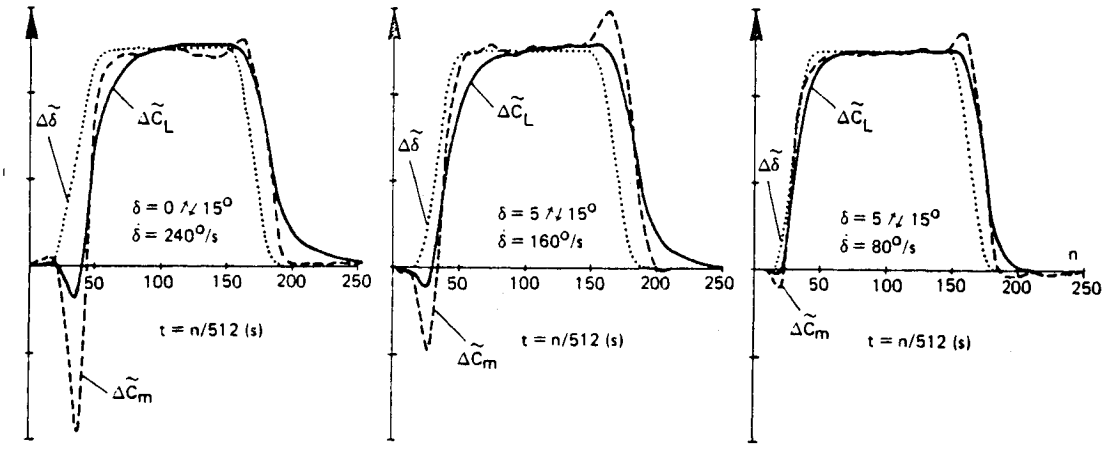

Fig. 19 Time histories of normalized increments of spoiler deflection $\Delta\delta$, lift ΔC_L, and pitch moment ΔC_M.

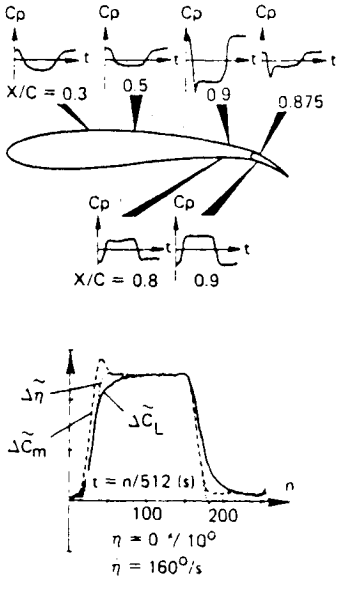

Fig. 20 Time histories for pressure distribution and normalized integrated coefficients for a flap ramp movement.

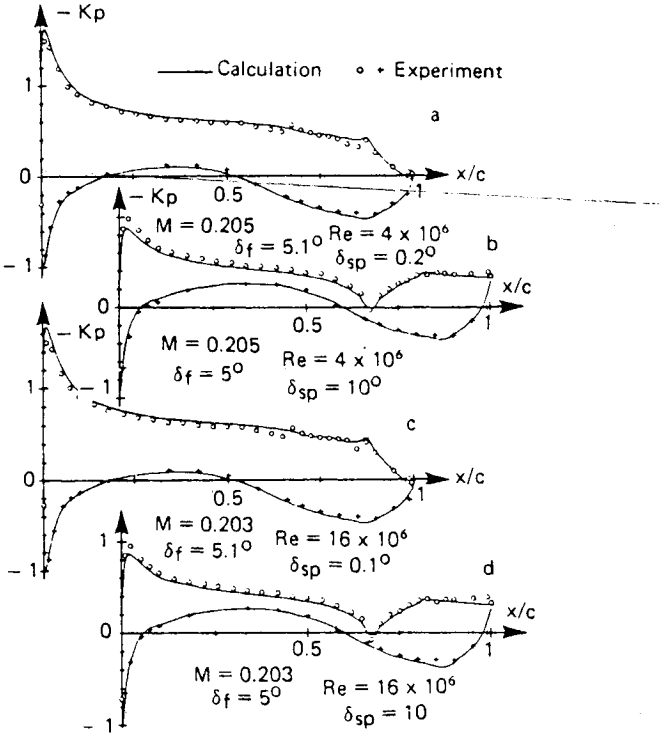

Fig. 21 Airfoil with spoiler; comparison calculation/experiment; influence of Reynolds number.

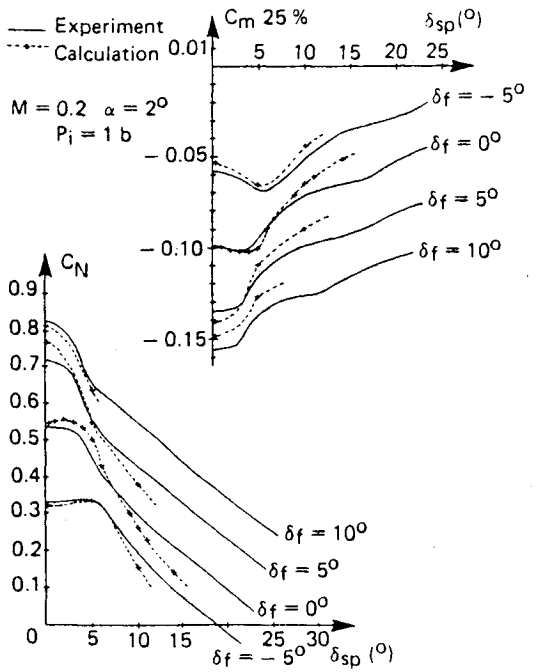

Fig. 22 Airfoil with spoiler and flap; comparison calculation/experiment; lift and moment evolutions.

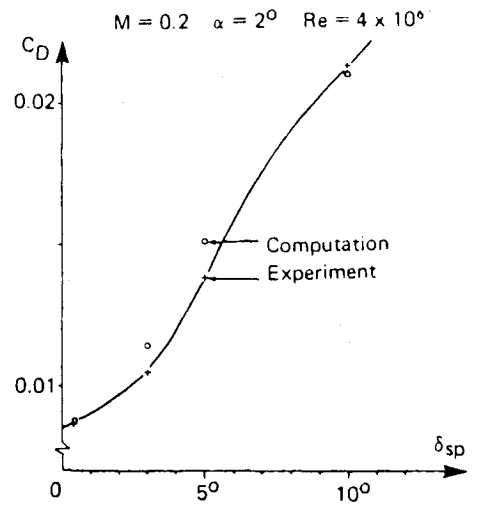

Fig. 23 Airfoil with spoiler; comparison calculation/experiment; influence of spoiler deflection on the drag coefficient.

agreement between the computed and experimental results is generally good. The region of no efficiency for small spoiler angles and its evolution with the flap angle are well predicted. However, in the linear region, the spoiler efficiency is overestimated by the computations. Figure 23 shows a comparison between the computed and experimental drag evolution vs the spoiler angle. The code that calculates the pressure and skin friction drags also predicts quite well the experimental airfoil drag as measured in the wake.

Conclusions

The tests performed in the ONERA F1 wind tunnel have made it possible to collect numerous and accurate data concerning the steady and unsteady flows around an airfoil equipped with a spoiler and flap. The results presented here have shown that the Reynolds number effect is very weak for this supercritical airfoil and, for the unsteady configurations, noticeable only when separated zone fluctuations can be observed on the airfoil (small spoiler deflections or/and great flap angles). The examination of spoiler and flap performances proves that, for this model, the spoiler efficiency can be higher than that of the flap, but with a significant phase lag penalty for the spoiler. It has also been observed that the steady and unsteady performances of the spoiler and flap evolve rapidly with their mean static angle when the spoiler angle is small. Because of this important interaction, great care must be taken in the control design. However, one hopes that these effects are smaller in realistic three-dimensional flows. Finally, ramp measurements have confirmed the much more nonlinear behavior of the spoilers already observed for harmonic oscillations. Furthermore, they have shown the overshoot phenomena specific to these transient movements. Computational results obtained with a two-dimensional viscous code using a strong coupling technique have proven the ability of this code to describe the very complex flow appearing when a spoiler is erected.

References

[1]Christoux, C. and Gravelle, A., "A Digital Unit for Measuring Unsteady Pressure Coefficients," *La Recherche Aérospatiale*, No. 1980-1 (English and French Edition), 1980.

[2]Le Balleur, J. C., "Calculation Method for Transonic Separated Flows over Airfoils Including Spoiler Effects," *Proceedings of the 8th ICNMFD, Aachen, Lecture Notes in Physics,* Springer-Verlag, New York, June 1982.

[3]Le Balleur, J. C., "Strong Matching Method for Computing Transonic Viscous Flows Including Wakes and Separations—Lifting Airfoils," *La Recherche Aérospatiale,* No. 1981-3 (English and French Edition), 1981, pp. 21–45.

[4]Destuynder, R., Barreau, R., and Anders, G., "Efficiency of Different Control Surfaces in Quasi Steady and Unsteady Motion Applications," *61th AGARD SMP Meeting,* Oberammergau, Germany, Sept. 1985.